Journal of Manufacturing Systems 43 (2017) 235–247

Contents lists available at ScienceDirect

Journal of Manufacturing Systems

journal homepage: www.elsevier.com/locate/jmansys

Technical Paper

High performance computing simulations to identify process parameter designs for profitable titanium machining

Mathew Kuttolamadom[a,*], Joshua Jones[b], Laine Mears[c], James Von Oehsen[d], Thomas Kurfess[e], John Ziegert[f]

[a] Texas A&M University, College Station, TX, United States
[b] Koyo Bearings USA LLC, Greenville, SC, United States
[c] Clemson University, Clemson, SC, United States
[d] Rutgers, The State University of New Jersey, Piscataway, NJ, United States
[e] Georgia Institute of Technology, Atlanta, GA, United States
[f] University of North Carolina at Charlotte, Charlotte, NC, United States

ARTICLE INFO

Article history:
Received 1 October 2016
Received in revised form 9 February 2017
Accepted 22 February 2017
Available online 16 March 2017

Keywords:
HPC simulations
Titanium machining
Finite-element
Automation
MRR
Tool wear

ABSTRACT

The objective of this paper was to conduct a study of the multi-level multi-variable design space in titanium machining through high performance computing (HPC) simulations that was otherwise too vast to be explored by physical experiments alone. For tool wear-based performance metrics, this resulted in a validated set of machining parameters for achieving profitable material removal rates (MRR) (optimized cost of processing and tooling) across multiple operational configurations, alloys, tool geometries, and process conditions. The approach was to include all machining-related variables and their distributions available within the software as inputs to finite-element models (FEM) of the machining process. The time intensiveness of conducting such large numbers of lengthy simulations was handled by wrapping Third Wave Systems AdvantEdge FEM machining simulation software with Dassault Systemes iSight to automate the building of experimental designs and their parallel execution on a HPC cluster. Results were analyzed using SimaFore software to identify key characteristics through bivariate analyses. A subset of simulations was validated through physical experiments, and these were in turn used to augment physically untested regions in the design space. Based on this, an MRR-based cost model for orthogonal turning was derived to drive optimal machining setups. This study showed the feasibility of integrating and automating a HPC loop involving the generation of suitable design of experiments (DOE), creating simulation jobs, deploying/executing it on a HPC cluster, and scripting outputs in a useful format. Besides highlighting the challenges in reading/transferring data across different software and in handling/compiling large amounts of data, this study also shed light on the need for benchmarking processor–operating system–software combinations for computational efficiency.

1. Introduction

1.1. Motivations and challenges

The overarching focus of this paper was to integrate software in a partially-automated loop to efficiently conduct a large number of simulations/analyses over a HPC cluster, in order to understand how to cost-effectively realize the most profitable MRR when machining titanium alloys. The motivations for this work were twofold. First was the need to map and understand the productivities involved when machining titanium alloys under various process conditions, from a profitability standpoint. The associated challenges involve the prohibitive nature of conducting a large number of physical experiments to explore the multi-level multi-variable design space due to the cost involved, and time/effort/resources needed. When considering the simulation route to explore this design space, a major hurdle encountered was the time intensiveness of conducting even a single machining FEA simulation on a high-end workstation (a typical job takes several hours to complete); this renders design space exploration via simulations using a high-end (stand-alone) workstation impractical from a time/effort standpoint. This leads us to the second motivation for this work, which is to leverage a HPC cluster to be

* Corresponding author at: Texas A&M University, 117E Thompson Hall, 3367 TAMU, College Station, TX 77843-3367, United States.
E-mail address: mathew@tamu.edu (M. Kuttolamadom).

http://dx.doi.org/10.1016/j.jmsy.2017.02.014
0278-6125/

able to explore and map the vast design space in order to identify profitable process parameter combinations for titanium alloy machining. Though the time intensiveness of running a large number of FEA simulations could potentially be mitigated via a HPC cluster, the major associated challenges involve being able to handle the large amount of input parameter data, the efforts involved in setting up these simulation jobs ready for submission to the cluster, and analyzing an even larger output dataset so that useful conclusions could be drawn in a timely manner. In order to address the challenges, a consolidated approach to setup, conduct and analyze a large number of machining FEA simulations was carried out in partnership with three commercial software; the major steps involved partially-automating the loop of creating DOE, deploying it into the FEA software to generate simulation jobs, running these on a cluster, and analyzing results.

1.2. Background and literature review

1.2.1. Titanium alloys – machining considerations/needs

The highly desirable material property combinations of titanium alloys such as its high strength-to-weight ratio and excellent corrosion resistance make it an attractive material alternative for many engineering applications. However, high raw-material and processing costs are major barriers to its widespread adoption. Efforts are underway for the development of cheaper grades to reduce raw-material costs and thus increase its use in certain commercial markets (*e.g.*, automotive) [1–8]. When considering the processing of titanium alloys, the machinability is generally poor, thus increasing processing cost via either extended cycle time (labor cost) or increased tool wear (tooling cost). This results in titanium alloys being classified as 'difficult-to-machine' materials, though it use in the commercial automotive industry could lead to significant savings in energy/life-cycle costs [9–11], except for low-volume batches [12–16]. The poor machinability of titanium alloys (especially the workhorse alloy, Ti–6Al–4V) is due to its unique combination of low thermal conductivity and elastic modulus along with high chemical reactivity and high temperature strength. As a result, even ultra-hard tool materials such Polycrystalline Diamond (PCD) and Cubic Boron Nitride (CBN) wear away often in an unpredictable manner; thus, from a net-cost standpoint, some of the most economical cutters still are 'throwaway' straight carbide inserts [17–19]. Though guidelines exist for machining titanium alloys [20–23], operating within the recommended range of process parameters still result in frequent and catastrophic wear. Thus, there is a critical need to explore the vast parameter design space when machining titanium alloys with carbide/other tools.

This calls for the simulation/mapping of the titanium machining process across the design space via HPC clusters. Sweeping the vast multi-variable multi-level design space through simulation will augment the knowledge that can be practically obtained by physical experiments. A better understanding of the dominant variables that affect tool life in titanium machining will be obtained via simulation results that span multiple configurations, alloys, tool geometries, and cutting conditions. Such validated (simulation-supported, with high degree of confidence) parameter designs will help drive process planning. Integrating data analytics software onto a machine tool controller will allow for visualization of the (evolving) variable sensitivities, and could provide close to real time control and optimization of the cutting process with the aid of feedback from force/temperature sensors.

1.2.2. Applicability of high performance computing to machining

High performance computing (HPC) in its simplest form refers to a cluster of processors working in parallel to provide significant computing power; its performance is dictated by the computing capacity of individual processors, their number, usage strategy, etc., as well as by the communication efficiency and data management between processors [24]. The computing resources could be in the form of dedicated clusters of processors, across a grid or a cloud [25]. When considering HPC applicability to machining, its much sought-after implementation-level of being able to analyze large volumes of in-process (sensed) data for close to real time control/optimization is still in its infancy. Currently, HPC use is limited to pre/post-event simulation/analyses of machining processes. Most commonly, these are either (FEA) simulations of the machining process or sensitivity analyses of sensed machining process output datasets. The performance of HPC clusters (in dedicated/grid/cloud configurations) for handling data-heavy FEA [26–32] jobs spanning a number of application areas, including machining specific FEA [33] has been detailed by numerous investigators. Additionally, it should be noted that although there have been numerous efforts in model-based or data-driven (*e.g.*, Bayesian) estimations of machining output parameters (such as force components or rudimentary measures of tool wear), there has not been a software-integration effort involving a HPC cluster for machining tool wear estimation so far.

1.3. Research gaps and future needs

Altogether, this scenario points to a number of research questions and gaps, especially in light of the recent advances made in big-data, automation, and cloud/mobile computing capabilities. First, given the current levels of computing powers readily accessible, there is a critical need to elucidate the fundamental behaviors within physical processes (such as machining), and to explore the process across its extended design spaces; in other words, there is the need (and capability) to now map and understand all possible aspects of a process, which was previously constrained by data volumes and/or computing resource needs. Next is the realization that the raw computing/processing power needed is just one of the components within a process flow loop, and that the capability to read/transfer and handle large volumes data is critical at every step. Question that arise include concerns on compatibility issues between software, data readability/transferability within the process flow loop, usability of the conclusions drawn, etc. This paper address these basic questions, and strives to conduct a software integration involving a HPC cluster.

2. Methodology

This project had two concurrent purposes. First, the integration and partial-automation of generating a suitable design of experiments (DOE), creating a large number of corresponding FEM simulation jobs, and deploying it onto the HPC server was successfully accomplished, in addition to scripting the large volume of simulation results to be output in a format readable by the data analytics software. And second, a detailed scrutiny of the multi-level multi-variable design space in machining titanium alloys from a profitability standpoint was enabled through (validated) simulations, which was otherwise not feasible to be explores via cutting experiments alone. The major steps involved are outlined below:

1. *Machining simulation design*: The first step was to formulate the experimental design of simulation runs, conduct trial runs for initial physical experiment validations, and to select the final subset of input and output variables relevant for analyses. For this, an initial assessment of comparative tool performance for a number of tool substrates was conducted. Then, a master list of all available input parameters in the Third Wave Systems AdvantEdge FEM simulator was compiled. Then, a subset of 12 variables and their respective ranges were selected. Similarly, a

master list of all available output parameters was compiled, and the subset of outputs to be analyzed, selected.
2. *Variability integration*: This step was to integrate Dassault Systemes iSight random variable wrapper onto AdvantEdge FEM software. For this, a number of candidate input matrices were generated, their design-space distributions analyzed, and a final input parameter matrix based off an Optimal Latin Hypercube-DOE of 100 runs, selected. Then, iSight was used to write AdvantEdge FEM input file sets corresponding to each of the 100 DOE setups to enable parallel computing runs.
3. *HPC integration*: This step integrated the FEM simulator onto the HPC cluster. For this, the AdvantEdge FEM simulator was installed on the HPC cluster, and design-space corners tested using Python script, resulting in mesh setting adjustments.
4. *HPC runs*: This step involved conducting multiple parallel simulations on the HPC cluster. For this, a number of machine configurations were benchmarked for computing times, and a suitable configuration was selected for the least computing time. Using this setup, all 100 runs were simultaneously completed on the HPC cluster in about 8 h, a task that would normally take about 800 h on a single high-performance PC having 4-cores.
5. *Bivariate analysis*: The simulation outputs (FEM model results) from the HPC cluster were then analyzed using SimaFore software for identifying key variables affecting titanium machining. By analyzing pairwise scatter plots, the key input variables that significantly affect the process were identified. Further, two derived variables, MRR and the tool wear rate were added as parameters onto the analyses set, and found to be key variables as well.
6. *Physical experimental validation*: The next step was to validate some of the simulation results through actual machining experiments using Okuma machine tools. A matching carbide insert was used to conduct these cutting experiments at key points in the design-space; maximum steady-state forces were compared for validation purposes. Further, OntoSpace software was employed to compare the model and experimental results in an effort to validate the credibility of the baseline FEM model.
7. *Control integration*: Finally, an MRR-based cost model was derived to drive optimal machining setups for maximizing profitability in titanium machining. This was deployed as the objective function of a real-time control algorithm aimed at satisfying a multi-objective optimization between cycle time and tool life for maximizing profitability. The results were measured against heuristic baseline values.

3. HPC-integration into simulation setups, and results

In order to accomplish the project objectives seven sequential task-sets were undertaken, as detailed below. Prior to their execution, preliminary assessments led to the following decisions:

- The Windows version of AdvantEdge FEM was selected for project use due to a larger body of knowledge and technical support available, over its counterpart Linux version.
- Preliminary integration of Isight and AdvantEdge was furthered by conducting trials of data transfer between the software (DOS executions, not using windows-based graphical user interfaces (GUI)).
- Assessments on using either High Throughput Computing (HTC) or HPC clusters were conducted. It was decided to run the Windows version of AdvantEdge FEM using virtual machines (VM) on the (Linux-based) HPC cluster.

3.1. (Step 1) – Machining simulation design

The first step involved formulating the experimental design of simulation variables, conducting trials for initial validations, and selecting a final subset of input/output variables for analyses from Third Wave Systems Advantage FEM machining simulation software. This is an explicit, dynamic, thermo-mechanically coupled FEM software specifically for machining process analysis, which uses physics-based process and material models to study the tool–chip–workpiece interfaces [34,35]. Model inputs include workpiece, tool, process and simulation-related parameters, while outputs include tool, workpiece, and chip temperatures, cutting forces, torque, power and workpiece quality characteristics such as residual stress, surface and sub-surface damage, and burr formation.

3.1.1. Tool performance assessment for comparing different substrates

One of the initial steps for the design of cutting simulations is to assess the comparative tool performance of different tool substrates to determine whether a carbide tool is an adequate choice for machining titanium alloys. Through a number of ultra-hard tool substrates (and coatings) such as Polycrystalline Diamond (PCD) and Cubic Boron Nitride (CBN) have been developed over the years for machining 'difficult-to-machine' materials, some of the most economical cutters for titanium still are the relatively cheap uncoated, straight "throwaway" carbide inserts [17–19]. The initial assessment of comparative tool performance was made based on the maximum steady-state (after the simulation/cut has stabilized) output forces and temperatures and their respective distributions. Table 1 lists the maximum cutting and feed forces and temperatures as simulated for the four selected tool substrates (carbide, ceramic, CBN and PCD with a high thermal conductivity (K)) when turning Ti–6Al–4V under recommended process conditions. Fig. 1(a) shows the temperature distribution on the carbide tool, and Fig. 1(b) shows the output forces, power and temperatures for a cutting distance of 10 mm. The process conditions used for the above preliminary simulations were a cut depth of 1 mm, feed of 0.15 mm/rev, cutting speed of 60.0 m/min, no coolant, initial temperature of 20 °C and a friction coefficient of 0.5. The tool geometry consisted of a rake angle of 5^0, relief angle of 10^0 and a cutting edge radius of 0.02 mm. The minimum and maximum adaptive element sizes were 0.02 mm and 0.1 mm respectively, resulting in 24,000 nodes.

As seen in Table 1, on assessing comparative tool performance through simulation, carbide tools were seen to experience cutting and feed forces comparable to or lower than other ceramic, PCD and CBN tools, thus substantiating their selection. Also, other than PCD, the temperatures were comparable as well. Note that the lower temperatures in PCD tools can be attributed to their

Table 1
Maximum steady-state (SS) forces and temperatures experienced by the four selected tool substrates.

Tool material	Max. (SS) cutting force	Max. (SS) feed force	Max. (SS) tool temp.
Carbide (general)	~280 N	~150 N	~800 °C
Ceramic (general)	~270 N	~140 N	~950 °C
CBN	~280 N	~160 N	~750 °C
PCD (high '*k*')	~325 N	~225 N	~250 °C

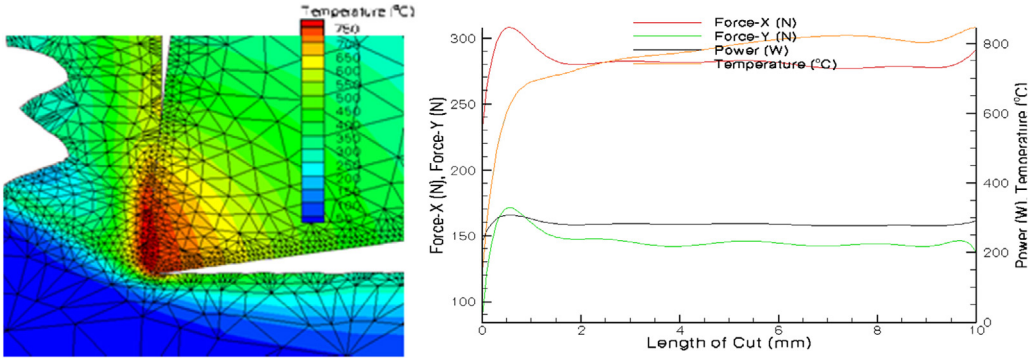

Fig. 1. (a) Temperature distribution on the carbide tool when turning Ti–6Al–4V and (b) filtered data of steady-state cutting force, feed force, power and temperature on the carbide tool.

combination of comparatively higher thermal conductivity (k), compressive strength and hardness, *i.e.*, ~560 W/m K, 7.6 GPa and 50 GPa for layered PCD vs. ~100 W/m K, 4.5 GPa and 13 GPa for (K10) tungsten carbide, respectively [36], in addition to their lower (dry) frictional coefficients (0.16), compared to tungsten carbide (0.32) or other ceramics (0.49 for Si_3N_4) [37]. This is especially relevant when machining Ti–6Al–4V (which has very low 'k' compared to common steels/Al-alloys) where a majority of the heat generated (as much as ~80% [38]) stays within the tool, and temperatures increase exponentially with velocity. As a result, the 'k' of the tool material significantly affects the eventual recorded temperatures in the cutting zone, illustrated by PCD tools resulting in lower maximum steady-state temperatures compared to carbides (250 °C vs. 800 °C) [39–41]. It should also be noted that Table 1 includes simulated force/temperature values for a constant frictional coefficient ($\mu = 0.5$), limited due to the friction-related options in the software.

3.1.2. Selected input parameters and their ranges

For generating the design of experiments, a master input parameter list of all available options in the FEM software was compiled, which falls under four categories: (i) *Workpiece inputs* such as stock height, length, initial stress, material, composite stock properties (number of layers/thickness); (ii) *Tool inputs* such as cutting edge radius, rake and relief angles and lengths, material, mesh parameters, wear model; (iii) *Process inputs* such as feed, cut depth, cut length, speed, initial temperature, friction coefficient, coolant; (iv) *Simulation inputs* such as mode, chip breakage, residual stress, and other mesh settings. From this master list, a multi-parameter subset input list was down-selected to serve as the input for Isight to generate the DOE. Each of the selected 12 variables was assigned 2 levels, a high and low level, and these were used as the bounds for generating suitable DOE designs (Table 2). Some of these had binary inputs such as the alloy type (Commercially Pure (CP) = 0, and Ti–6Al–4V = 1), and coolant condition (Off = 0 and On = 1). Note that the coolant condition "Off" negated the effects some of its sub-variables. It should be mentioned that since a large number of simulations could be conducted without additional expense of significant time/resources, the design space was extendable beyond the standard recommended ranges of (input) parameters, and their distributions within this range could be made quite dense (beyond what is practically feasible through physical experiments alone). This afforded the opportunity to test extreme tool/process combinations as well without fear of tooling/equipment loss or damage.

3.1.3. Selected output parameters and their ranges

In a similar manner, a master output parameter list of all available outputs in the FEM software was compiled. This includes steady-state maximum values (over each time step) of cutting and feed forces, power, torque, and temperature. Further, at every (x,y) location of the tool and workpiece (for each time zone) the following outputs are available: temperature, heat rate, plastic strain and rate, Mises stress, pressure, Maximum shear stress, maximum and minimum principal stress, and velocities. From these, feed and cutting forces and temperature were used initially for establishing correlations with the input variables. Also, two derived variables, MRR and Usui model wear rate were calculated. The effects of feed, speed and cutting depth are captured in the MRR, and pressure, velocity and temperature are used in the calculation of the Usui wear rate. Also, since power is directly derived from cutting forces, it need not be additionally accounted for. Two candidate stress-related outputs, Von-Mises stress and the principal stress were also analyzed. Von-Mises stress in an indicator of plastic flow, and principal stress of abrasive wear in the simulation.

Table 2
2-Level subset of selected input parameters that served as bounds for their ranges.

#	Menu	Input parameter	0	1
			Upper and lower bounds	
1	Workpiece	Alloy type	CP	Ti–6Al–4V
2	Tool	Cutting edge radius (mm)	0.01	1
3	Tool	Rake angle (degrees)	−5	20
4	Tool	Relief angle (degrees)	5	15
5	Process	Feed (mm/rev)	0.05	0.25
6	Process	Depth of cut (mm)	0.5	3
7	Process	Cutting speed (m/min)	30	120
8	Process	Workpiece initial temperature (°C)	20 °C (room)	100 °C
9	Process	Coolant	Off	On
10	Process	Coolant heat transfer coefficient	10000 W/m^2 K	20000 W/m^2 K
11	Process	Coolant temperature (°C)	20 °C (room)	60 °C
12	Process	Coolant location	Exclude tip	Focused

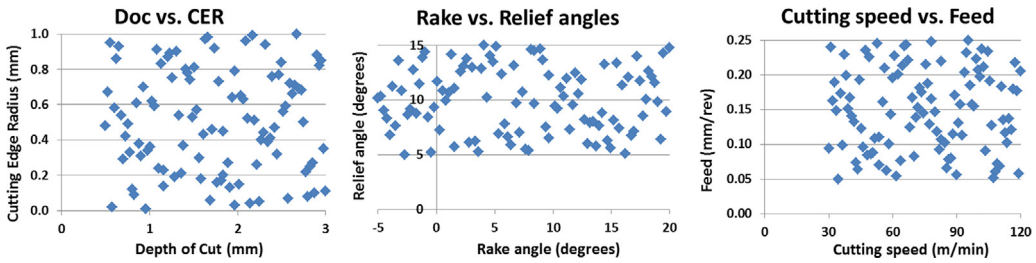

Fig. 2. Distribution of depth of cut (DoC) vs. cutting edge radius (CER), rake vs. relief angles, and cutting speed vs. feed in the 100-run OLHC DOE.

3.2. (Step 2) – Variability integration

The second step involves integrating Dassault Systemes iSight random variable wrapper onto AdvantEdge FEM to create a large number of simulation jobs to run in a parallel HPC environment. Isight is an integration/automation software for creating simulation process flows across programs, automating their execution, and exploring the resulting design space.

3.2.1. Generating the input parameter DOE

To account for all 12 selected input parameters, a number of DOE matrices were generated and explored. Among these, a 100-run DOE generated via an Optimal Latin Hypercube (OLHC) was selected that provided a good spread of continuous variables (*e.g.*, cutting edge radius varying from 0.01 to 1 mm) as well as a suitable variation of the discrete variables (alloy type). Other DOE generated/considered include a 448-run DOE matrix (generated via a 7-level Latin Hypercube for continuous variables and a Full Factorial 2-level matrix for discrete variables), a 112-run DOE matrix (generated via a 7-level Latin Hypercube matrix for continuous variables and Orthogonal Array of a 2-level matrix for discrete variables), etc., which could be used for future studies.

Isight was used to generate input decks for the FEM software by using the OLHC technique to generate the parameter matrix. The OLHC technique is a modified Latin Hypercube where the combination of factor levels for each factor is optimized, rather than randomly combined and the design space for each factor is divided uniformly. These levels are randomly combined to generate a random Latin Hypercube as the initial DOE design matrix with n points. An optimization process is applied to the initial random Latin Hypercube design matrix, and a new matrix is generated and the new overall spacing of points is evaluated. The goal of this optimization process is to design a matrix where the points are spread as evenly as possible within the design space defined by the lower and upper level of each factor. The distribution of cutting depth vs. tool edge radius, rake vs. relief angle, and cutting speed vs. feed in this generated DOE are given in Fig. 2 respectively. This OLHC DOE design evenly covers the whole design space and is thus used to capture the effects of the variables.

3.2.2. Generation of AdvantEdge FEM input files by Isight

Isight workflow (Fig. 3) is used to pass input parameter values into AdvantEdge input files. The workflow contains several Data Exchanger (DatEx) components that are used for file parsing and recoding the files. Most of the files have same structure for all AdvantEdge runs so that different combinations of input parameter values could be passed to such files by only modifying parameter values in DatEx components. The only exception was the project file *.twp that had slightly different structure for different coolant delivery locations. To address this challenge, three different file templates were used and processed accordingly for different coolant delivery locations using “Data Exchanger”, “Exclude Tip”, and “Focused” DatEx components.

The DOE execution results in creating 100 folders that have different names and same set of input AdvantEdge files that have different content updated during file parsing in Isight runtime. In this manner, the input parameters of all 100 runs of the generated DOE were imported into corresponding input files of AdvantEdge FEM by using Isight script. Starting with a customized representative set of input files, they were modified as dictated the DOE for each of the 100 runs. For instance, the string “*process0.5,0.0,5.0E-5,5.0E-4,0.0030 20.0*” in the “*.INP” file, sets the cutting speed = 0.5 m/s, feed = 5.0E−5 m/rev, depth of cut = 5.0E−4 m, and initial temperature = 20 °C. A total of five file types had to be modified for each run, namely, *.twt files (tool information), *.inp files (process information), wp.twm files

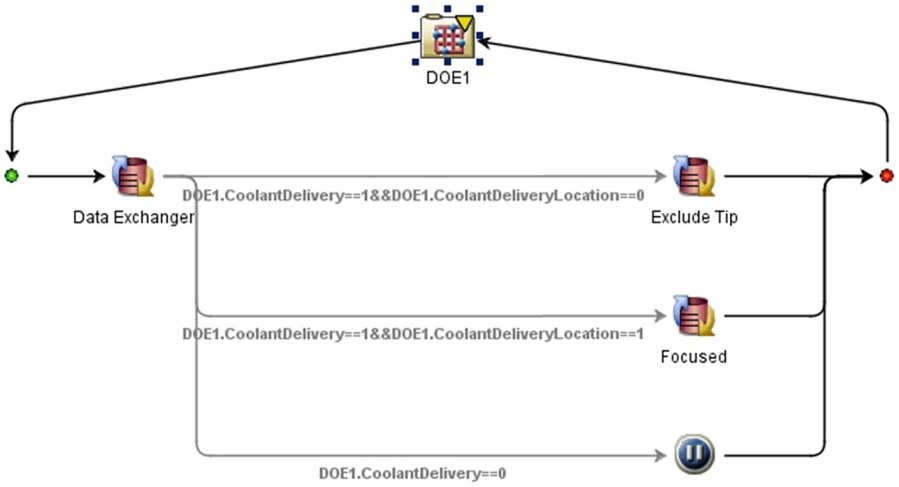

Fig. 3. Isight workflow that can handle different input file format requirements of the FEM software.

Table 3
Mesh settings updated from default to Iter-5 configuration.

	Default	Iter-5
Workpiece parameters		
Max. elem. size (mm)	0.1	0.01
Min. elem. size (mm)	0.02	0.005
Cutting radius fraction	0.6	0.6
Feed fraction	0.1	0.1
Mesh refining factor	2	4
Mesh coarsening factor	6	4
Tool parameters		
Max. elem. size (mm)	0.1	0.02
Min. elem. size (mm)	0.02	0.005
Mesh grading	0.4	0.4

(workpiece material information), *.tww files (workpiece information) and *.twp files (information to be displayed on GUI).

3.3. (Step 3) – HPC integration

The third step involved integrating the wrapped AdvantEdge FEM simulator onto a HPC cluster to enable concurrent parallel runs, testing the corners of the design space, and making mesh adjustments. The HPC Palmetto cluster is a Linux-based 'condominium' style supercomputer resource at Clemson University having over 14,000 cores (1627 nodes), and a performance of 100+ trillion floating-point operations per second (teraFLOPS). It was #6 among US academic institutions, and #96 worldwide as of June 2011's list of Top 500 Supercomputing Sites [42].

3.3.1. Design space corner runs for mesh setting refinements

Due to the aggressive re-meshing needed within AdvantEdge FEM, which mirrors the actual machining operation for titanium alloys, the mesh and simulation settings needed to be checked for its capability in handling these aggressive mesh updates. For this, sample simulations were conducted on the feed-speed design space corners to confirm successful completion of the runs. Following a number of trials with finer mesh settings, a much more refined mesh setting (*Iter-5*) was decided on, as given in Table 3.

Following trail runs using the above refined mesh settings (*Iter-5*), a number of additional refinements were made such as increasing the length of cut to allow for the better temperature stabilization, and modifying the output file format writing instructions to enable easier extraction of data. After re-generating the 100-run DOE with these modifications, and the corresponding FEM software input file sets (11 files per run in each of the 100 folders, for a total of 1100 files), two sample runs were conducted on a standalone machine; these two simulations (run 1, run 100) completed successfully as shown in Table 4.

3.3.2. Integration of AdvantEdge FEM onto the HPC cluster

Because AdvantEdge is a Windows based application and the Palmetto cluster is a Linux based system, AdvantEdge FEM software was installed on a Windows Virtual Machine (VM), and submitted as a HPC job. A VM is a software implementation of a computer with a complete system platform, in this case, a Windows platform. For this a kernel-based virtual machine (KVM) was used, which is a Linux kernel module that allows to utilize the virtualization features of many processors as well as QEMU, which is a generic and open source machine emulator and virtualizer. KVM and QEMU together create a framework for creating and running VM on a cluster. Once the Windows Server VM was created, AdvantEdge FEM was installed. In addition, Python was installed for implementing a start-up script, that enabled to specify the location of the input directories, location of executables, SSH key to allow password-less login back onto the cluster, and location on the cluster for saving results, among others. This script was used to run all 100 simulations simultaneously and when submitted, all 100 VM would boot up and start running AdvantEdge FEM, each as a different simulation.

3.4. (Step 4) – HPC runs

The fourth step involved running the 100 simulations on a HPC cluster concurrently. For this, computing times wear benchmarked to select a configuration with least computing time and all 100 runs were simultaneously completed on the HPC cluster in about 8 h, a task that would normally take about 800 h on a single high-performance PC having 4-cores.

3.4.1. Benchmarking simulation times (local machine vs. cluster configurations)

As a first step, simulation tests were conducted to determine the best combination of the processor–operating system–software bit (32/64), in terms of expended time vs. computing resources. For this, an initial benchmarking of the computation times needed for a high-end local machine against different HPC system configurations was done. A 2D turning simulation with wear computation turned off (Fig. 4) was conducted on (i) a Sun Microsystems Workstation (Windows 7, 64 bit, 4 cores, 16 GB RAM) and (ii) VM on the Palmetto Cluster (8, 16 core configurations). Though the VM on the cluster could engage 24-cores, the maximum number that AdvantEdge FEM (for the version used) could engage was limited to 16 cores, and hence used. It was noted that computation run times do not 'linearly' decrease with an increasing number of parallel cores; output is dependent on the speed of data transfer between processors.

The next step was to compare the computing times needed for each processor–operating system–software (32/64 bit) combination. For this, the maximum 'steady-state' cutting and feed forces, and temperatures experienced during the simulation were compared for the results from the standalone local machine vs. the HPC cluster configurations. It was found that results were similar across hardware setup types. However, a 64-bit software version (and OS) on a 64-bit processor was found to have the least computing time

Table 4
Simulation times on a standalone machine for runs #1 and #100 for confirming successful simulation completions before forwarding all 100 jobs to the cluster.

0.135	0.103	f (mm/rev)
Run 1: **[Ti-6Al-4V]** *Cutting edge radius: 0.42mm* *Rake angle: -1.46* *DoC: 0.727mm* *Coolant: On* CPU time: 35h 4 cores: 11h	***Run100:*** **[CPTitanium]** *Cutting edge radius: 0.08mm* *Rake angle: 9.65* *DoC: 2.798mm* *Coolant: Off* CPU time: 28h 4 cores: 8.25h	
111.84	113.64	V (m/min)

```
Case 1: 2D Turning, Wear simulation = Off, Tool type = Standard
Sun Microsystems Workstation (Standalone PC) [64 bit/ 4 cores/ 16 GB]
Elapsed CPU Time: 31777.67s (8h 49min 37.67s)
Actual elapsed Time: 9652.00s (2h 40min 52.00s)

Virtual Machine on Palmetto cluster (HPC) [8 cores]
Elapsed CPU Time: 23843.23s (6h 37min 23.23s)
Actual elapsed Time: 4592.00 s (1h 16min 32.00s)

Virtual Machine on Palmetto cluster (HPC) [16 cores]
Elapsed CPU Time: 47724.39 s (13h 15min 24.39s)
Actual elapsed Time: 4107.00 s (1h 8min 27.00s)
```

Fig. 4. Computing times for a 2D turning simulation with wear computation turned off.

(as expected). The combination was used throughout the project for all simulation runs.

3.4.2. Simultaneous HPC runs of the doe and compilation of outputs for post-processing

Following benchmarking, the DOE of 100 runs was simultaneously run on the cluster by constructing exclusive VM for each input setup. A single run takes approximately 9 h on a quad-core machine running Windows Server 2008 R2 SP1 so it would take 900 h on a single desktop machine. By moving to a HPC environment, all 100 simulations were simultaneously run to complete in about 8 h.

Each of the simulation results from the 100-run DOE was first checked for successful completion. Only 5 out of the 100 runs had errors, leaving 95 good runs. These five setups could be re-run with a finer mesh setting for completion. From these 95 good runs, the maximum values of temperature, cutting force, feed force, and power were extracted from each simulation's "*.ft.tec" output file. Discussions on which value (in each parameter data file) needs to be selected, took place between the project partners, *i.e.*, whether to choose the very last data point value of each parameter's last time step, values at a stabilized time step, maximum of filter-forced data values, or maximum stabilized data point value of each parameter. Plots of the variation of forces and temperatures with time for run #1 are shown in the form of raw data (Fig. 5(a)), and filter-forced values (Fig. 5(b)). Fig. 6 shows the distribution of temperature and Von-Mises stress on the carbide tool and Ti–6Al–4V workpiece for Run #1 respectively. Relevant process parameters include a cut depth of 0.73 mm, feed of 0.13 mm/rev, cutting speed of 111.8 m/min, focused coolant with a heat transfer coefficient of 10 kW/m^2 K at a temperature of 20 °C, initial Ti–6Al–4V workpiece temperature of 100 °C and a friction coefficient of 0.5. The tool geometry consisted of a rake angle of −1.46°, relief angle of 11.46° and a cutting edge radius of 0.42 mm.

From these plots, it was concluded that due to the chip segmentation (saw tooth type chip as a result of adiabatic shear banding) common in Ti–6Al–4V machining, the filtered data (Fig. 5(b)) should not be used, and that either the last data point value or the maximum stabilized value of each parameter should be compiled for further analysis from the raw data plots (Fig. 5(a)). Accordingly, the very last data point value of each parameter (last entry in the "*.ft.tec" output file), as well as the maximum stabilized value (gauged manually on a case-by-case basis), for each of the 95 completed simulation runs, was compiled for comparison. From these, it is noted that force, temperature, and power generally were in agreement except for a few extreme cases; both these output result sets were forwarded for SimaFore. Additionally, a separate benchmarking exercise that used Advantage FEM software on another HPC cluster for simulations involving drilling, indexable and solid tooling can be found in [35].

3.5. (Step 5) – Bivariate analysis

The fifth step involves analyzing the simulation outputs using SimaFore software for identification of key significant variables affecting profitability in the titanium machining process. SimaFore is a data analytics tool that uses bivariate analysis to identify significant variables by measuring the information exchange ratio (IER) in each plot, and to perform variable sensitivity analyses.

3.5.1. Bivariate analysis (#1) of process inputs and direct outputs

The main objective of performing the information exchange ratio (IER). Bivariate analysis was to detect key factors of influence using data from Monte Carlo simulations (MCS). IER helped to short list a subset of variables which account for the most information within the MCS dataset and thereby helped in identifying critical process variables. In this case, starting with 12 input and 4 output variables, a full bivariate analysis resulted in 120 pairwise scatter plots. The % contribution of each variable to the total IER was computed, and resulting variables were ranked by the amount of information exchange loss that resulted if that particular variable was removed. The results of the analysis indicated that four output variables account for a significant amount of information within the dataset as indicated in Table 5. Loss of any of the top four output variables would result in a loss of nearly 35% or higher

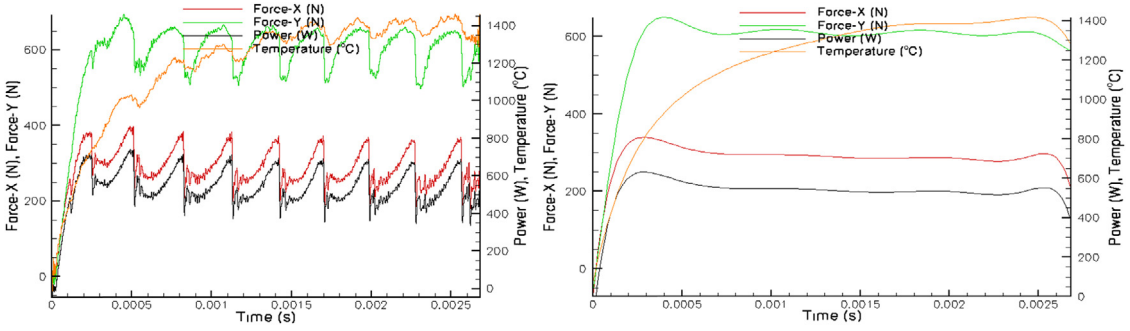

Fig. 5. Variation of forces, temperatures, and power for run #1: (a) raw data and (b) filtered data.

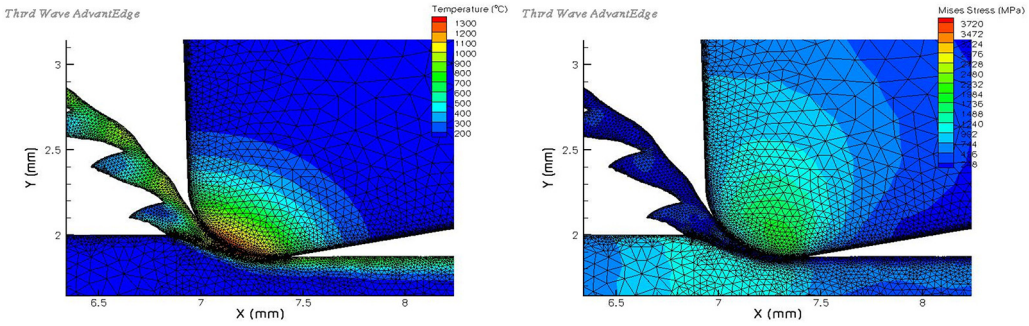

Fig. 6. Distribution of (a) temperature and (b) Von-Mises stress on the tool and workpiece for run #1.

Table 5
Bivariate analysis results considering standard inputs and outputs.

Variable	% IER loss if removed	Rank	Type
Force *X*	42	1	Output
Force *Y*	40	2	Output
Temperature	38	3	Output
Power	36	4	Output
Titanium alloy type	33	5	Input
Cutting speed	4	6	Input
Cutting edge radius	4	7	Input
Depth of cut	3.5	8	Input

Table 6
Bivariate analysis results considering derived outputs.

Variable	% IER loss if removed	Rank	Type
o3. Force *Y*	37.30%	1	Output
o6. Mises stress	35.61%	2	Output
o2. Force *X*	34.32%	3	Output
i12. Titanium alloy type	32.23%	4	Input
d2. Usui wear rate	19.60%	5	Derived
i4. Cutting edge radius	12.29%	6	Input
d1. MRR	12.25%	7	Derived
i10. Rake angle	10.00%	8	Input

information. The choice of the titanium alloy was the most significant input variable, accounting for 33% of total IER. Cutting speed (4%), cutting edge radius (4%) and depth of cut (3.5%) were the only other input contributors within the dataset.

Fig. 7 shows the circle connect map for run #1, and an inset bivariate plot of maximum principal vs. shear stress. Here, all important variables are arranged in a circle, with the most important at the 12 o'clock position. The connecting line thickness is proportional to the interconnection strength, and clicking it opens up associated bivariate plots. As an illustration, on the 'parent' connect map (not shown), whose information is summarized in Table 5, when probing the connecting line between temperature (output) and titanium alloy type (input), the bivariate plot shown in Fig. 8 opens up, showing distinct clusters for alloy type, *i.e.*, CP vs. Ti–6Al–4V.

Thus, from this analysis, the four primary *output variables* that contributed to the maximum % IER loss were ranked as force-*X* direction, force-*Y* direction, temperature and power. And, the most significant *input variables* from the simulation results were ranked as titanium alloy type, cutting speed and cutting edge radius. These identified variables ranked consistently between the "last-data point" and "maximum stabilized value" set of analysis results; this was expected as variation between datasets was fairly small.

3.5.2. Bivariate analysis (#2) of process inputs and derived outputs

The IER analysis was repeated by adding two additional variables to the data matrix: wear rate and material removal rate (MRR). These variables were calculated from existing factors used in the MCS, no new HPC run was performed. IER analysis indicated that output factors still dominate the total information exchanged in the dataset, and titanium alloy type was still the most significant input parameter. The derived factors accounted for 12–20% of the information and hence were not insignificant. A notable difference in this analysis was the influence of rake angle was noticed which was previously missing from the list of significant factors (Table 6). In summary, besides the three primary output variables (two forces, and Von-Mises stress), the most significant input and derived variables and their % IER losses, in the order of significance are titanium alloy type (32% IER loss if removed), Usui wear rate (20%), Cutting edge radius (12%), MRR (12%), and Rake angle (10%).

3.5.3. Conclusions from the two bivariate analyses

In the above two bivariate analyses, the primary outputs that were used for ascertaining input variables' significance were the force-*x* (cutting force), force-*y* (feed force), and temperature. These three outputs were consistently ranked highest; this suggests the significant amount of information exchange associated with these output variables, as well as the fact that the selected input variables significantly affect these outputs. Further, values of these three outputs are the primary variables used for comparing tool performance as well as representing tool wear; hence, their high ranking based on % IER loss is logical.

When considering inputs, choice of the titanium alloy type was the most significant input variable, accounting for about 33% of the total % IER loss. This was expected due to the significant difference in material properties between the two grades; grade-5 titanium (Ti–6Al–4V) has more than double the (tensile) strength of grade-2 titanium (CP), as well as about one-third of its thermal conductivity, and hence very differentiable resulting forces and temperatures. In the analysis with standard process inputs and outputs, cutting speed and tool cutting edge radius were the other two significant input contributors; increasing cutting speeds and tool edge radii resulted in higher output forces and temperatures as shown in Fig. 9(a) and (b). These identifications and behaviors conform to prior known guidelines [20–23] for machining titanium alloys, specifically, lowering effective surface speeds and using very sharp tools.

Further, in the second bivariate analysis with derived process inputs and outputs, the idealized wear rate and MRR were identified as significant contributors to tool deterioration as quantified by maximum steady-state interfacial temperatures. The direct dependence of temperature with MRR thus substantiates its selection as a control variable as opposed to surface speed alone.

3.5.4. Conclusions from regression analyses

In addition to the above SimaFore analyses, the dataset was subjected to multiple linear regression and best subsets regression

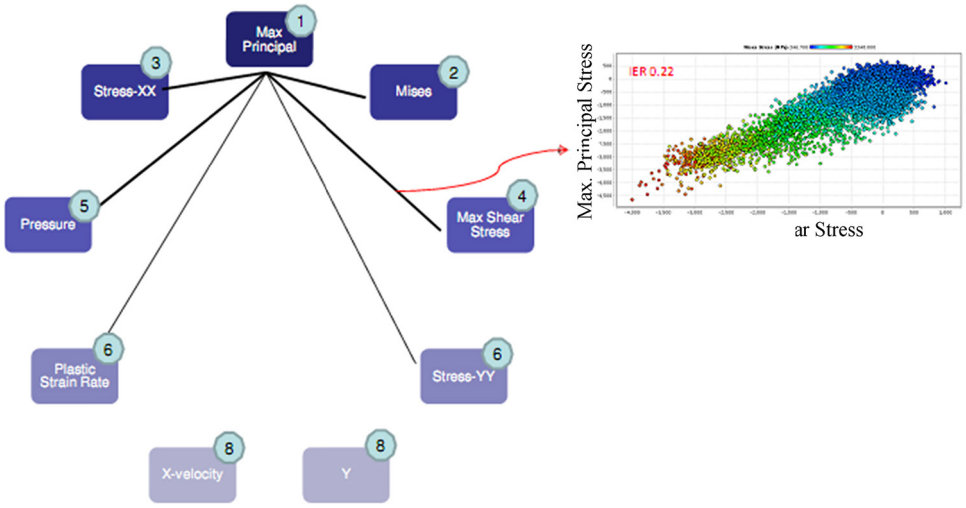

Fig. 7. Connect map for run #1 with bivariate plot of maximum principal stress vs. maximum shear stress.

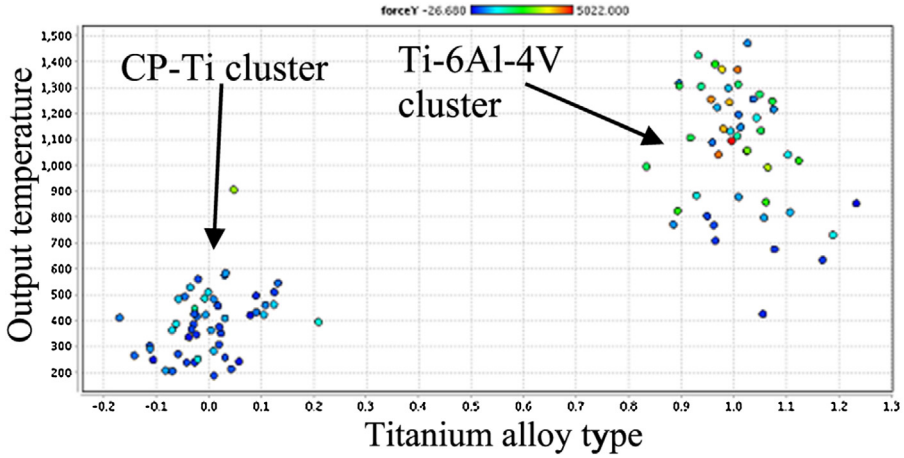

Fig. 8. Bivariate plot of temperature vs. titanium alloy type, where *x*-axis is alloy type, *y*-axis is temperature, and color range denotes force (*y*) range. (For interpretation of the references to color in this figure legend, the reader is referred to the web version of the article.)

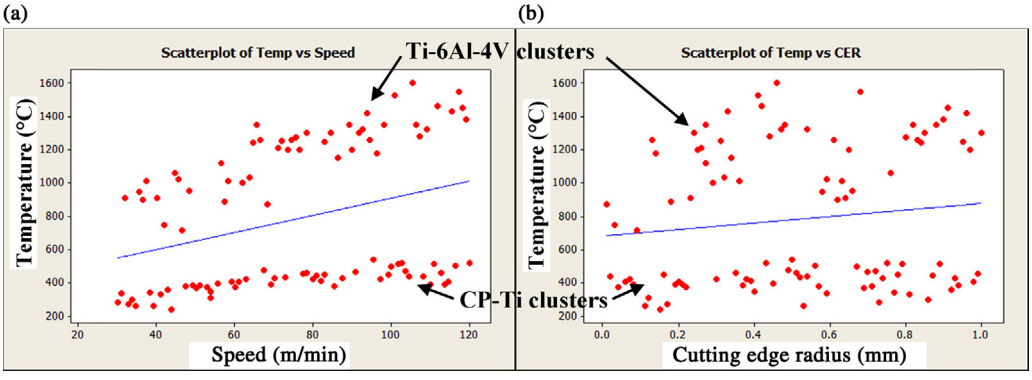

Fig. 9. Scatter plot of temperature distribution for Ti alloys for (a) surface speed and (b) cutting edge radius.

analyses in Minitab to identify significant variables. Main conclusions include:

- The alloy type was the most significant factor on considering all runs and the three outputs.
- The cutting edge radius was the next significant input variable when considering the forces, while surface speed was the significant variable when considering temperature for both grades.
- Beyond these three input variables, the other significant variables were the cutting depth and feed rate; thus, all three constituents of MRR have been identified as significant.

Next, the input–output dataset was subjected to best-subsets regression analyses. As before, besides the alloy type emerging as the most significant input variable, cutting edge radius was found to be significant for the cutting/feed forces, while, surface speed

was found to be significant for temperature. Again, the next two significant variables turned out to be the depth of cut and feed, thus constituting all MRR terms.

A note on the potential effect of the design space extent on parameter significance is apt at this point. In machining studies, there might be certain parameters that end up being more dominant within certain operational ranges, especially when extending the design space beyond standard recommended ranges of (input) parameters. For instance, when operating at 'extreme' limits of cutting edge radii, this parameter might overshadow the effects of other typical dominant parameters such as cutting velocity, feed rate, etc. Thus, it might be beneficial to simulate within parts of the design space as well as all together. The paper's primary purpose was to automate a large number of HPC simulations across an extended design space study. Even with this vast range, it confirmed (and did not contradict) well-known conclusions.

3.6. (Step 6) – Physical experiment validation

The sixth step was to conduct a series of cutting trials using an instrumented machining center to validate a subset of the cutting simulation results. For this, an uncoated straight carbide insert (Sandvik CNMG 12 04 08-QM H13A) was chosen, and its geometry and material parameters (obtained from Sandvik) input into of AdvantEdge FEM software. Relevant tool parameters include an 80° diamond insert shape, relief angle of 0°, inscribed circle of 0.5″, negative rake and a nose radius of 0.8 mm. The machining center used was an OKUMA Space Turn LB4000-EX turning center and force sensing was conducted using a calibrated strain-gage based sensor integrated turning tool holder.

3.6.1. Validation #1: 12-run DOE with generic tool geometry

As a first step for validating the simulation results, a parameter matrix of 12 runs was set up within the recommended range of feed-speed parameters for turning grade-5 titanium. The purpose was to check whether the simulation results conformed to known machining trends. For this initial validation study, the 12 cases were successfully simulated in AdvantEdge FEM. For each feed-speed combination, maximum steady-state temperatures, forces and power values were compiled. The simulation results for dependence of cutting and feed forces with feed rate are shown in Fig. 10.

The tool used for these simulation runs was a standard uncoated carbide (grade-K) tool with generic tool geometry. For these dry (no coolant) simulation runs, the trends in forces and temperatures were in conformance to known machining behavior and no anomalies were observed; this serves as a first-step validation of the simulation results.

3.6.2. Validation #2: 9-run DOE simulation with matching tool geometry

In this final validation step, maximum steady-state force values (cutting and feed forces) were compared for a 9 run DOE in the recommended feed-speed design space, for simulation results and counterpart physical cutting experiments. Input-file sets were created using this tool type, and forwarded to the HPC cluster for job runs. All nine runs were completed successfully on the cluster with an average computation run time of about 8 h. It was observed seen that both the simulated and predicted force values followed similar increasing trends with cutting feed (Fig. 11). The actual maximum steady-state force values were slightly lower than the predicted force values, especially at higher feed rates. These forces seemed to not be affected by surface speed significantly – this is in conformance with the conclusions from the earlier regression analysis where cutting and feed forces were primarily dependent on cutting edge radius and feed, while temperature was primarily dependent on the surface speed.

3.7. (Step 7) – Control integration

The final step was to derive an MRR-based cost model to drive optimal machining setups for profitability in titanium machining. This model opens the potential to be deployed as the objective function of a real-time control algorithm aimed at satisfying a multi-objective optimization for profitability.

3.7.1. MRR-based cost model

Traditional process optimization is essentially done by optimizing the cutting speed for a right balance between too long of a machining time (labor cost) and too many tool changes (tooling cost). However, it is know that the sudden and unexpected catastrophic tool wear and failure events that are very common in Ti–6Al–4V machining, are a direct consequence of the high interfacial temperatures which are an exponential function of surface speed. This fact limits the surface speeds usable during titanium machining; hence, a surface speed-based time and cost optimization of the titanium machining process is not the best way to go. This is where MRR offers itself as a viable control and productivity parameter. Besides being the eventual productivity objective of all machining studies, note that by adopting MRR as the control variable, surface speeds can be limited, but the feeds and depth of cuts can be appropriately increased to maintain the same MRR. MRR for orthogonal turning operations is defined in the form:

$$MRR = V \cdot f_r \cdot d \tag{1}$$

where V is the cutting speed in mm/min, f_r is the feed in mm/rev, and d is the depth of cut in mm, for obtaining MRR in mm^3/min. Also, the maximum idealized wear rate (based on Usui's wear rate model) is:

$$\dot{W}_{Usui} = Ke^{\alpha/(T+273)}pV \tag{2}$$

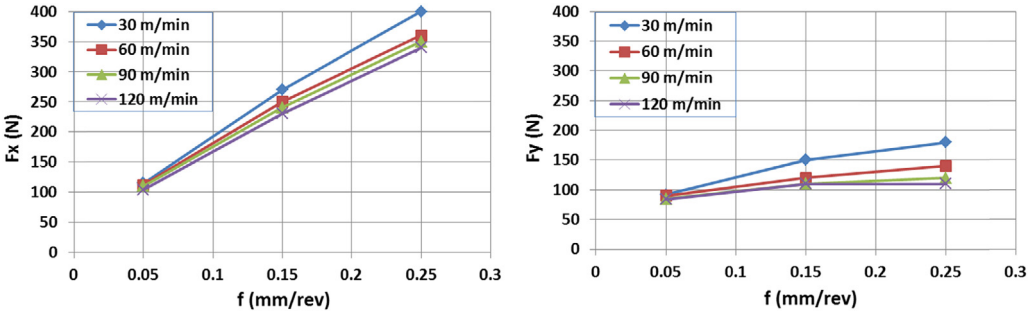

Fig. 10. Maximum steady-state cutting and feed forces increasing with feed rate.

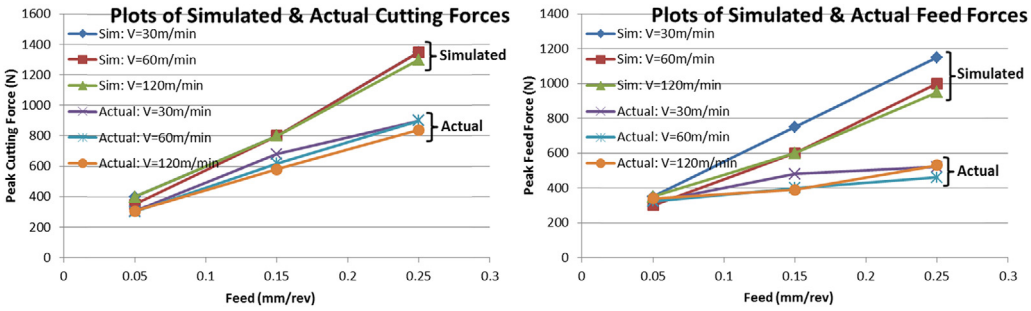

Fig. 11. Plot of simulated and actual cutting forces (Fx) and feed forces (Fy).

where T is the temperature in °C, p is the pressure in MPa, V is the surface sliding velocity magnitude in m/min, K is a constant with a unit of Pa^{-1}, and α is a constant with a unit of Kelvin, to obtain the resultant Usui wear rate in mm/min. The constants K and α have the values 7.8×10^{-9} Pa^{-1} and 2500 K respectively for the case of Ti–6Al–4V being cut by a carbide tool. Based on these two derived variables, a machining cost model was formulated which was essentially a cost-based objective function dependent on the opposing constraints of MRR and wear rate, in the following form:

$$f(\$) = \frac{c_1}{MRR} + c_2 \dot{W}_{Usui} \tag{3}$$

where f is the objective function to be minimized, $\dot{W}_{Usui}$ is the maximum idealized wear rate (based on Usui's wear rate model), and c_1 and c_2 are constants. Note that this generic functional form is essentially the rate extension of the traditional speed-based (V) productivity maximization between shorter cycle times (*time*) and too many tool changes (*flank wear*).

On plotting the above computed cost-objective function for all simulation runs for both the titanium alloys (Fig. 12), the total machining cost was found to be high for the lowest MRRs (due to a decrease in material-removal productivity). Also, the reduction in cost leveled-off as well as started to slightly increase with higher MRR (due to increasing tool wear rate). Though the opposing effects of the idealized wear rate were small in this model compared to the more dominant effect of material-removal productivity on cost, an argument can be made that in reality, combining other relevant factors into cost such as the extended labor cost, tool changing cost, etc., the costs will increase with higher MRRs. Note that, this plot also included a number of diverse alloys (with drastically different material properties), coolant conditions being on and off (significantly affecting the process mechanics), etc. Thus, such a formulation provides a startup point for MRR-based cost modeling in machining titanium alloys.

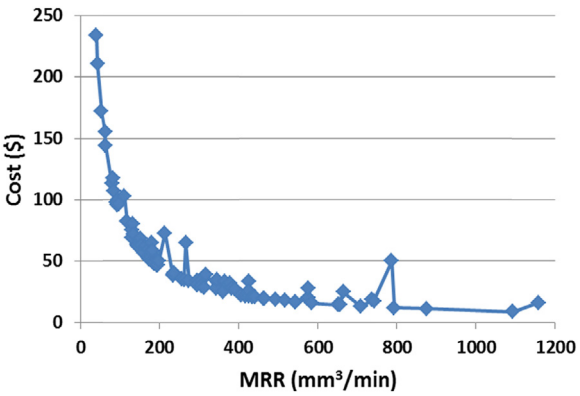

Fig. 12. Cost-based objective function against the MRR.

3.7.2. Control algorithm for profitability

Machining process modeling and control is aimed toward gaining a better understanding of the physical phenomena, optimization of some objective (wear minimization and/or MRR maximization), and rejection of disturbances (variation in input part quality). Some of the applications of Model Based Control (MBC) for machining processes include machining chatter control [43,44], cutting force prediction/control [45,46] and controlling the deflection of slender workpieces during turning operations [47–49]. Based on the insights gained from this work, one can apply the developed model, (i) first for process parameter selection (process planning) and (ii) then for incorporation into a model-based control of the machining process for maximizing profit. In this approach, the control variable will be the MRR, and the control algorithm will act to minimize this cost function by changing the MRR (feed, depth of cut, and capped surface speed) for a balance between maximized material removal with good tool life.

4. Conclusions

This project primarily involved the software integration of a partially-automated loop for generating a suitable DOE, creating simulation jobs, deploying it onto a HPC cluster, and outputting results in a usable format. The field of application was the FEA simulation of titanium alloy machining with tool wear-based performance metrics. By following the methodology outlined, common-sense technical conclusions were reached that were consistent with the state-of-the-art knowledge in the field, thus demonstrating its technical merit. Using a HPC cluster-integrated software loop enabled the analyses of a multi-level multi-variable extended design space of titanium machining simulations that was not feasible to be explored via physical experiments alone. This project highlighted the challenges involved and the need for seamless integration between different software, particularly from data-transfer/readability standpoints, and the substantial initial efforts often needed for integrating software and computing resources within a loop. The ability to handle large volumes of input and output data between software, as well as to rapidly derive useful results from such disparate datasets (big data) turned out to be a critical factor for success. In addition, flexibility to retool/iterate within the loop proved essential as well; for instance, the higher temperature regimes involved in real titanium-alloy machining required simulated cutting length and mesh size adjustments in between runs without compromising the large job set. Further, benchmarking processor–operating system–software version combinations for computational efficiency, as well as accounting for potential computing platform incompatibilities (*e.g.*, Windows vs. Linux) was needed.

5. Future work

Some of the future work that could be pursued as a result of extending this project's results includes:

- Developing dedicated HPC routines for machining FEA simulation. This project helped clarify the computational efficiency regimes of the FEA software; this could be leveraged to improve software performance.
- Further exploration of machining tool-insert parameters for understanding tool wear. Only a limited subset of tool geometries was explored in this project; these could be further expanded.
- The 2D setup that was explored could be extended to 3D simulation. This is especially useful with a HPC resource, as the computational load grows exponentially with an added dimension.
- Tool wear exploration. The simulations utilized a classical wear model that considered only one wear mechanism. Models could be augmented/combined for more realistic wear predictions.

Funding

This work was supported by the U.S. Department of Energy (DOE) – National Energy Technology Lab (NETL) and by the National Center for Manufacturing Sciences (NCMS): Lightweight Automotive Materials Program (LAMP).

Acknowledgements

Don O'Brien, Malik Kayupov, Dassault Systemes SIMULIA Corp., Detroit, MI

Hari Elangovan, Dan Munoz, Third Wave Systems, Eden Prairie, MN

Bala Deshpande, SimaFore, Ann Arbor, MI

Okuma America Corporation

American Titanium Works

Sandvik

Clemson Computing & Information Technology (CCIT) Center

References

[1] Froes FH, Yu K, Nishimura T. Developing applications for titanium. In: Cost-affordable titanium symposium dedicated to Professor Harvey Flower. The Minerals, Metals & Materials Society; 2004. p. 19–26.
[2] Faller K, Froes FH. Titanium in automobiles. In: Materials and science in sports. The Minerals, Metals & Materials Society; 2001. p. 47–56.
[3] Faller K. Management justification to select titanium automotive components. In: SAE technical paper 2002-01-0363, SAE 2002 world congress. 2002.
[4] Froes FH, Gungor MN, Imam MA. Cost-affordable titanium: the component fabrication perspective. J Miner Met Mater Soc 2007;6:2028–31.
[5] Sagara M, Takayama I, Nishida T. Application of titanium for automotive use in Japan. In: Nippon steel technical report no. 62; July 1994. p. 1923–8.
[6] Sherman AM, Allison JE. Potential for automotive applications of titanium alloys. In: 860608, SAE technical paper series. 1986.
[7] Yamashita Y, Takayama I, Fuji H, Yamazaki T. Applications and features of titanium for automotive industry. In: Nippon steel technical report no. 85; January 2002. p. 2011–4.
[8] Leyens C, Peters M. Titanium and titanium alloys: fundamentals and applications. Weinheim, Germany: Wiley-VCH; 2003.
[9] Kuttolamadom MA, Jones JJ, Mears ML, Ziegert JC, Kurfess TR. A systematic procedure for integrating titanium alloys as a lightweight automotive material alternative (2011-01-0429). In: SAE 2011 world congress. 2011.
[10] Kuttolamadom MA, Jones JJ, Mears ML, Kurfess TR, Funk K. Life-cycle integration of titanium alloys into the automotive segment for vehicle light-weighting: Part II – Component life-cycle modeling & cost justification (2012-01-0785). In: SAE 2012 world congress. 2012.
[11] Jones JJ, Kuttolamadom MA, Mears ML, Kurfess TR, Funk K. Life-cycle integration of titanium alloys into the automotive segment for vehicle light-weighting: Part I – Component redesign, prototyping, & validation (2012-01-0784). In: SAE 2012 world congress. 2012.
[12] Kosaka Y, Fox SP, Faller K, Reichman SH. Development of low cost titanium alloy sheets for automotive exhaust applications. In: Cost-affordable titanium symposium dedicated to Professor Harvey Flower. The Minerals, Metals & Materials Society; 2004. p. 69–76.
[13] Keller MM, Jones PE, Porter WJ, Eylon D. The development of low-cost TiAl automotive valves. J Miner Met Mater Soc 1997;(May):1942–4.
[14] Dowling WE, Allison JE, Sherman AM. The development of γ/α2 titanium aluminides for exhaust valves. In: Titanium'92. The Minerals, Metals & Materials Society; 1993. p. 2681–8.
[15] Froes FH, Faller K. The use of titanium in family automobiles: current trends. J Miner Met Mater Soc 2001;53(4):27–8.
[16] Jette PSA. Titanium for automotive racing. In: Titanium for energy and industrial applications; 1981. p. 199–215.
[17] Defense USDo. Titanium and titanium alloys: military handbook (MIL-HDBK697A); 1974.
[18] Donachie MJ. Titanium: a technical guide. Materials Park, OH: ASM International; 2000.
[19] Ezugwu EO, Wang ZM. Titanium alloys and their machinability – a review. J Mater Process Technol 1997;68(3):262–74.
[20] Dieter G. Mechanical metallurgy. New York, NY: McGraw-Hill; 1986.
[21] Jaffery S, Mativenga P. Assessment of the machinability of Ti–6Al–4V alloy using the wear map approach. Int J Adv Manuf Technol 2009;40(7):687–96.
[22] Lim SC, Ashby MF. Overview no. 55 Wear-Mechanism maps. Acta Metall 1987;35(1):1–24.
[23] Shaw MC. Metal cutting principles. Cambridge, MA: MIT Press; 2004.
[24] Allcock B, Bester J, Bresnahan J, Chervenak AL, Foster I, Kesselman C, et al. Data management and transfer in high-performance computational grid environments. Parallel Comput 2002;28(5):749–71.
[25] Foster I, Zhao Y, Raicu I, Lu S. Cloud computing and grid computing 360-degree compared. 2008 grid computing environments workshop 2008.
[26] Wu D, Liu X, Hebert S, Gentzsch W, Terpenny J. Performance evaluation of cloud-based high performance computing for finite element analysis (57045); 2015. p. V01AT02A043.
[27] Annamalai V, Krishnamoorthy CS, Kamakoti V. Adaptive finite element analysis on a parallel and distributed environment. Parallel Comput 1999;25(12):1413–34.
[28] Mackerle J. FEM and BEM parallel processing: theory and applications – a bibliography (1996–2002). Eng Comput (Swansea, Wales) 2003;20(3–4):436–84.
[29] Huang W, Tafti DK. A parallel adaptive mesh refinement algorithm for solving nonlinear dynamical systems. Int J High Perform Comput Appl 2004;18(2):171–81.
[30] Wu D, Liu X, Hebert S, Gentzsch W, Terpenny J. Democratizing digital design and manufacturing using high performance cloud computing: performance evaluation and benchmarking. J Manuf Syst 2017;43:316–26.
[31] Mongelli M, Roselli I, De Canio G, Ambrosino F. Quasi real-time FEM calibration by 3D displacement measurements of large shaking table tests using HPC resources. Adv Eng Softw 2016.
[32] Ari I, Muhtaroglu N. Design and implementation of a cloud computing service for finite element analysis. Adv Eng Softw 2013;60–61:122–35.
[33] Man X, Usui S, Jayanti S, Teo L, Marusich TD. A high performance computing cloud computing environment for machining simulations. Procedia CIRP 2013;8:57–62.
[34] Stephenson DA, Bandhyopadhyay P. Process-independent force characterization for metal-cutting simulation. J Eng Mater Technol 1997;119(1):86–94.
[35] Marusich TD, Ortiz M. Modeling and simulation of high-speed machining. Int J Numer Methods Eng 1995;38:3675–94.
[36] ASM. ASM specialty handbook: tool materials. Materials Park, OH: ASM International; 1995.
[37] Divakar R, Blau PJ, Erosion ACG-o, Wear. Wear testing of advanced materials. American Society for Testing Materials; 1992.
[38] Konig W. Applied research on the machinability of titanium and its alloys. In: Proc AGARD conf advanced fabrication processes. 1979.
[39] Schrock DJ, Kang D, Bieler TR, Kwon P. Phase dependent tool wear in turning Ti–6Al–4V using polycrystalline diamond and carbide inserts. J Manuf Sci Eng 2014;136(4):041018.
[40] Tomac N, Tønnessen K, Rasch FO, Mikac T. A study of factors that affect the build-up material formation. In: Kuljanic E, editor. AMST'05 advanced manufacturing systems and technology: proceedings of the seventh international conference. Vienna: Springer; 2005. p. 183–92.
[41] Davim JP, Maranhão C, Jackson MJ, Cabral G, Grácio J. FEM analysis in high speed machining of aluminium alloy (Al7075-0) using polycrystalline diamond (PCD) and cemented carbide (K10) cutting tools. Int J Adv Manuf Technol 2008;39(11):1093–100.
[42] Palmetto cluster; 2017.
[43] Moradi HM. Sliding mode control of machining chatter in the presence of tool wear and parametric uncertainities. J Vib Control 2009;16(2):231–51.
[44] Zhang HJ. Spindle speed variation method for regenerative machining chatter control. Int J Nanomanuf 2009;3(1–2):73–99.
[45] Ibaraki AM. Monitoring and control of cutting forces in machining processes: a review. Int J Autom Technol 2009;3(4):445–56.
[46] Altintas Y. Prediction of cutting forces and tool breakage in milling from feed drive current measurement. J Eng Ind 1992;114:386–92.
[47] Benardos P, Mosialos S, Vosniakos G. Prediction of workpiece elastic deflections under cutting forces in turning. Robot Comput Integr Manuf 2006;22:505–14.

[48] Fan C, Collins E. Control design for a bar turning process using laser-based measurements. In: American control conference. 2000.
[49] Mehta P, Mears ML. Model based prediction and control of machining deflection error in turning slender bars. In: Proceedings of the ASME international Manufacturing Science and Engineering Conference (MSEC 2011). 2011.